Title

Simultaneous suppression of As mobilization and N2O emission from NH4 +/As-rich paddy soils by combined nitrate and birnessite amendment

Authors

Wang, Feng

Zhang, Jing

Hu, Jiehua

et al.

Publication Date

2024-03-01

DOI

10.1016/j.jhazmat.2024.133451

Peer reviewed

Journal of Hazardous Materials 465 (2024) 133451

Contents lists available at ScienceDirect

Journal of Hazardous Materials

journal homepage: www.elsevier.com/locate/jhazmat

Research Paper

Simultaneous suppression of As mobilization and N_2O emission from NH_4^+/As-rich paddy soils by combined nitrate and birnessite amendment

Feng Wang [a,1], Jing Zhang [f,1], Jiehua Hu [c], Honghui Wang [f], Yanqiong Zeng [a], Yanhong Wang [d], Peng Huang [a], Huanhuan Deng [a], Randy A. Dahlgren [a,e], Hui Gao [a,b,**], Zheng Chen [a,f,*]

[a] School of Public Health & Management, Wenzhou Medical University, Wenzhou 325035, PR China
[b] Key Laboratory of Fertility Preservation and Maintenance of Ministry of Education, Ningxia Medical University, Yinchuan 750004, PR China
[c] Department of Marine Biology, Xiamen Ocean Vocational College, Xiamen, Fujian 361100, PR China
[d] State Key Laboratory of Biogeology and Environmental Geology, China University of Geosciences, Wuhan 430074, PR China
[e] Department of Land, Air & Water Resources, University of California, Davis, CA 95616, USA
[f] School of Environmental Science & Engineering, Tan Kah Kee College, Xiamen University, Zhangzhou 363105, PR China

HIGHLIGHTS

- Combined nitrate-birnessite treatment decreased As(III) mobilization and N_2O emission from flooded paddy soils.
- Birnessite stimulates anoxic oxidation of ammonia and suppresses denitrification.
- Nitrate facilitates regeneration of MnO_2, thereby suppressing As(III) mobilization and N_2O emission.
- The combined treatment has good prospects for remediating As pollution and N_2O emission from paddy soils.

GRAPHICAL ABSTRACT

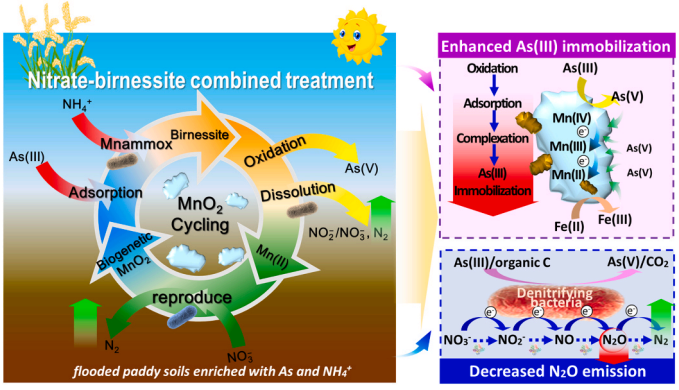

ARTICLE INFO

Editor: Edward Burton

Keywords:
Arsenic
Nitrous oxide
Nitrate
Birnessite
Flooded paddy soils

ABSTRACT

The environmental impacts of As mobilization and nitrous oxide (N_2O) emission in flooded paddy soils are serious issues for food safety and agricultural greenhouse gas emissions. Several As immobilization strategies utilizing microbially-mediated nitrate reducing-As(III) oxidation (NRAO) and birnessite (δ-MnO_2)-induced oxidation/adsorption have proven effective for mitigating As bioavailability in flooded paddy soils. However, several inefficiency and unsustainability issues still exist in these remediation approaches. In this study, the effects of a combined treatment of nitrate and birnessite were assessed for the simultaneous suppression of As(III) mobilization and N_2O emission from flooded paddy soils. Microcosm incubations confirmed that the combined treatment achieved an effective suppression of As(III) mobilization and N_2O emission, with virtually no As(T)

** Correspondence to: Key Laboratory of Fertility Preservation and Maintenance of Ministry of Education, Ningxia Medical University, Yinchuan, P.R. China.
* Correspondence to: School of Public Health and Management, Wenzhou Medical University, Wenzhou, P.R. China.
E-mail addresses: gh2010@126.com (H. Gao), chenzheng_new@163.com (Z. Chen).
[1] These authors were considered as the co-first authors.

https://doi.org/10.1016/j.jhazmat.2024.133451
Received 17 September 2023; Received in revised form 25 November 2023; Accepted 3 January 2024
Available online 5 January 2024

released and at least a 87% decrease in N_2O emission compared to nitrate treatment alone after incubating for 8 days. When nitrate and birnessite are co-amended to flooded paddy soils, the activities of denitrifying enzymes within the denitrification electron transport pathway were suppressed by MnO_2. As a result, the majority of applied nitrate participated in nitrate-dependent microbial Mn(II) oxidation. The regenerated biogenetic MnO_2 was available to facilitate subsequent cycles of As(III) immobilization and concomitant N_2O emission suppression, sustainable remediation strategy. Moreover, the combined nitrate-birnessite amendment promoted the enrichment of *Pseudomonas*, *Achromobacter* and *Cupriavidu,* which are known to participate in the oxidation of As (III)/Mn(II). Our findings document strong efficacy for the combined nitrate/birnessite treatment as a remediation strategy to simultaneously mitigate As-pollution and N_2O emission, thereby improving food safety and reducing greenhouse gas emissions from flooded paddy soils enriched with NH_4^+ and As.

1. Introduction

Arsenic (As) pollution in paddy soils is of great concern as a global food safety and human-health issue [31], particularly in regions consuming a diet rich in rice (e.g., Asia and Latin America). In flooded paddy soils, microbes play a key role in regulating the mobilization and speciation of As by regulating As-integrated biogeochemical cycles, such as C, N and Fe [9,24]. Due to long-term flood irrigation, paddy soils commonly experience sustained anoxic conditions, which fosters microbial reductive dissolution of As(V)/Fe(III)-bearing minerals that leads to elevated As(III) levels in anoxic layers [38]. Owing to the higher As(III) mobility, phytoavailability and toxicity compared to As(V) [11], the elevated As(III) levels are readily taken up by rice plants, thereby creating a serious food safety concern. Developing effective, environmental friendly and economically feasible methods to mitigate As(III) mobilization have become an urgent need for remediating As-polluted paddy soils.

Among a variety of As-immobilization remediation strategies, microbially-mediated nitrate reducing-As(III) oxidation (NRAO) is considered an effective approach to alleviate the bioavailability and toxicity of As in flooded As-polluted paddy soils [53]. The input of nitrate under anoxic conditions promotes microbial oxidation of As(III) to As(V) with concomitant denitrification reactions [53]. During the denitrification process, nitrate is ultimately reduced into molecular nitrogen (N_2) through a pathway producing intermediate gaseous nitrogen oxide products (e.g., nitric oxide (NO) and N_2O) as nitrate is utilized as a terminal electron acceptor by denitrifers [30]. The aforementioned soil denitrification process is the primary source of atmospheric N_2O [45]. N_2O results from incomplete denitrification in paddy soils and is a potent greenhouse gas having a global warming potential ~310 times that of CO_2 [42]. Thus, conventional remediation relying solely on NRAO-based biotechnology in paddy soils will inevitably trigger an opposing environmental impact, wherein the desirable As(III) immobilization (positive) effect is offset by intensified greenhouse gas production (negative) resulting in N_2O emission. Hence, it is essential to develop an ameliorative strategy utilizing NRAO-based biotechnology that simultaneously reduces As(III) mobilization and N_2O emission in paddy soils.

The intimate interactions between microbes and minerals in natural soils/sediments are of fundamental interest, as their complex interplay holds the key to understanding and altering integrated elemental cycling at a variety of temporal and spatial scales [15]. Manganese oxides (MnO_x) are a ubiquitous component of soils occurring at relatively high contents (>100 mg Mn/kg) [22]. In flooded anoxic soils, MnO_x (Mn^{3+}/Mn^{4+}) actively participates in the biogeochemical cycling of As and N. For instance, many natural/synthetic MnO_x are capable of oxidizing As(III) in the pH range generally encountered in aquatic environments (e.g., pH≈5–9) [49]. MnO_x can act as a direct electron acceptor for anoxic ammonium (NH_4^+) oxidation (denoted as Mnammox) by Mn-reducing bacteria to produce N_2, similar to anammox and Feammox [13]. This infers that the input of MnO_x could simultaneously reinforce denitrification-derived As(III) immobilization and attenuate N_2O emission via the Mnammox pathway (promoting generation of N_2) in NH_4^+/As-rich paddy soils. This postulation led us to posit that a combined nitrate-MnO_x amendment might be a feasible solution that could simultaneously suppress As(III) mobilization and N_2O emission in NH_4^+/As-rich paddy soils. To date, the effects of a combined nitrate-MnO_x amendment on suppressing As(III) mobilization and N_2O emission in flooded paddy soils remain unexplored, thereby warranting further exploration. Hence, there is a critical need to elucidate the interactive mechanisms associated with a combined nitrate-MnO_x amendment in paddy soils.

Combined pollution from elevated As(III) release and N_2O emission is common in flooded NH_4^+/As-rich paddy soils [20]. Remediation relying solely on NRAO-based biotechnology does not effectively address the opposing environmental impacts of As(III) mobilization versus N_2O emission. Hence, we proposed an ameliorative strategy for NRAO-based biotechnology that combines nitrate and MnO_x amendments. Birnessite (δ-MnO_2) is a naturally formed, amorphous MnO_x that is commonly found in soils [25]. In this work, we selected birnessite as a representative MnO_x model and focused on the effects of a combined nitrate-birnessite amendment on As(III) immobilization and N_2O emission in flooded paddy soils having high background concentrations of ammonia and arsenic. The main objectives of this work were to: (1) examine the synergistic effects of the combined nitrate-birnessite amendment on enhancing As(III) immobilization, (2) investigate N (bio)transformations using ^{15}N isotope tracing, and (3) elucidate the biological mechanism(s) associated with the simultaneous suppression of As(III) mobilization and denitrification. Results of this study provide new insights into practical remediation strategies to address food safety and greenhouse gas emissions from As-polluted paddy soils.

2. Methods and materials

2.1. Soil sampling and soil physicochemical properties

As-polluted soils were collected in June 2022 from an irrigated paddy field located in Shimen County (29°58′ N, 111°38′ E) in Changde City, Hunan Province, China. Soil cores (25 ×25 ×10 cm^3) were collected at the peak rice tillering stage from the 20–30 cm depth using a soil corer, then uniformly mixed to form a single composite sample. After being transported to the laboratory on ice, the fresh (undried) soil was stored at 4 °C in the dark before soil characterization analysis and initiation of incubation experiments. A subsample was dried at room temperature and sieved through a 2-mm mesh for the analysis of soil physicochemical properties (see Method S1). The paddy soil used for experiments was a typical acidic (pH=5.8), red clay soil with high contents of total As (79.2 ± 6.6 mg/kg) and oxidizable As (60.7 ± 8.1 mg/kg). Additional soil physicochemical characteristics are provided in Table S1. Notably, the paddy soil sample was highly enriched with NH_4^+-N (0.41 ± 0.08 g/kg).

2.2. Synthesis of birnessite

Synthesis of birnessite (δ-MnO_2) was conducted according to previously reported protocols [5]. In brief, 61.6 g KOH, 14.85 g $MnCl_2{\cdot}4\ H_2O$ and 3.95 g $KMnO_4$ were in turn dissolved into 125, 125 and 250 mL of Milli-Q water. Next, the prepared KOH and $MnCl_2$ solutions were mixed

in a 500 mL beaker for deoxygenation by N_2 bubbling for 3 min and then fully mixed with the $KMnO_4$ solution by magnetic stirring for 30 min. The resulting suspensions were then dried at 60 °C for 14 h. The precipitates were separated by removing the supernatant and washed with Milli-Q water until the filtrate pH reached 9–10. Thereafter, the resulting mixture was centrifuged at 12,000 rpm for 10 min to remove the supernatant and dried at 60 °C for 6 h. Finally, the dried particles were ground to pass a 100-mesh sieve. Scanning electron microscopy (SEM) and X-ray diffraction (XRD) were employed to confirm the characteristics of the birnessite particles (shown in Fig. S1a-b).

2.3. Soil microcosm experiments

All microcosms were conducted in 105-mL sealed serum bottles. Dissolved oxygen was evacuated by purging with helium for 60 min (liquid phase for 30 min and head space for 30 min). All microcosms were incubated at 30 °C in the dark. Following the experimental design of a previous investigation [24], dissolved As(III) was directly added into microcosms to examine As(III) immobilization under simulated, flooded As(III)-rich soil conditions. Briefly, each experimental microcosm was incubated with 12.0 g paddy soils (<2 mm), 36.0 mL of a given autoclaved reaction solution (5.0 mM acetate, 0.1 mM As(III), and with/without 10.0 mM δ^{15}N-nitrate) and 0.06 or 0.10 g birnessite. Herein, ^{15}N-labelled sodium nitrate (δ^{15}N–$NaNO_3$, 99% ^{15}N atom%; Aladdin, USA) was incorporated into the reaction solutions to trace N redox transformations. To block Mn-anammox reactions due to the direct contact of birnessite particles and soil microbes [13], the 0.06 or 0.10 g of birnessite and 2.0 mL of the given reaction solution (which comprised 5.0 mM acetate and 0.10 mM As(III)) were sealed in a semi-permeable dialysis bag (molecular weight cutoff: 14000 Daltons). The dialysis bag allowed the exchange of released metal ions and electrons but prevented direct contact between the birnessite particles and microbes. The sealed semi-permeable dialysis bags were placed on top of the soil and incubated in the aforementioned microcosms (Fig. 1a). A treatment without the addition of δ^{15}N-NO_3^- and birnessite was designated as the control (CK) group.

Prior to incubation, the reaction solutions and birnessite particles were autoclaved for 20 min at 120 °C to inactivate foreign microbes. All experimental operations were performed in an anoxic glove box and performed in triplicate. A detailed experimental design is provided in Table S2. In this work, we conducted a 8-d incubation to assess As(III) mobilization and N_2O emission processes. During the 8-d incubation, an aliquot of the supernatant (2.0 mL) was extracted from each microcosm at given intervals (1, 2, 4, 6 and 8 days) with a sterilized syringe, filtered through a 0.22 μm filter (nylon, Jinteng Co., China) and acidified with 1% HNO_3 prior to analyses for As, Fe, Mn and N species. At the end of the

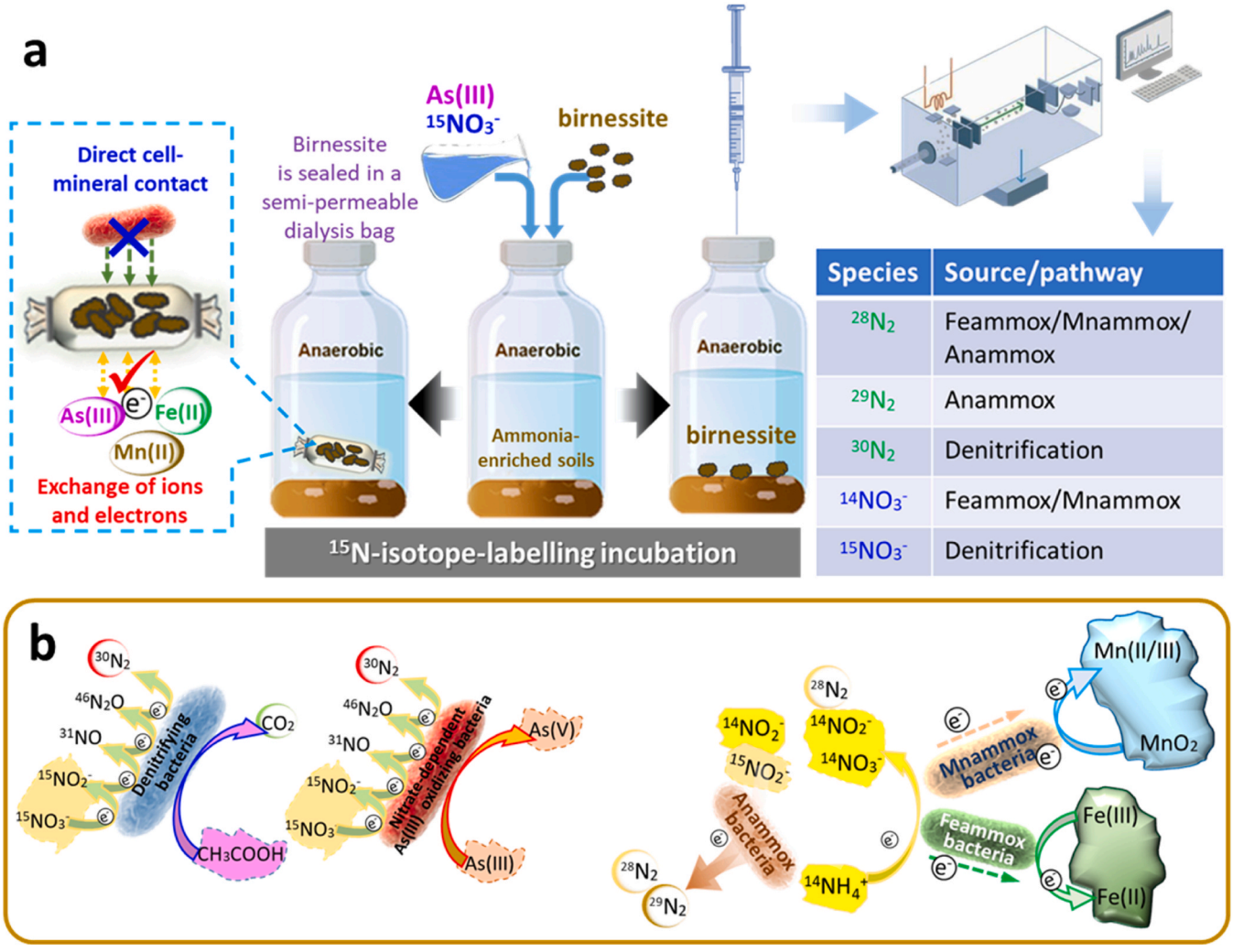

Fig. 1. Schematic of experimental setup for flooded paddy soil microcosms (a). The experimental amendments were conducted along with incubating together with ^{15}N isotope-labelled nitrate and birnessite (direct or indirect contact). Therein, the abundances of ^{15}N/^{14}N-derived NO_3^- and N-gas species were examined to identify different N transformation pathways (b). The reaction equations associated with specific biological N redox transformations incorporating ^{15}N/^{14}N-labelled components are listed in Table S3.

incubation period, the birnessite from the dialysis bags was separated to determine the speciation of adsorbed As/Fe by XPS (Quatum-2000, USA) [16].

2.4. Analytical methods

2.4.1. Determination of As/Fe/Mn species

Concentrations of dissolved Fe(T) (total iron) and Fe(II) in the supernatant of microcosms were determined using a UV–VIS spectrophotometer and phenanthroline colorimetric method (UV-2802, UNICO, China) [11]. The concentration of Fe(II) was determined without the addition of hydroxylamine hydrochloride, whereas Fe(III) concentration was computed by difference: Fe(III) = Fe(T) - Fe(II). The concentration of Mn(II) was quantified using the spectrophotometric method based on the oxidation of Mn(II) to MnO_4^- by potassium periodate [19]. Concentrations of As(T) (total arsenic) and Mn(T) (total manganese) were determined using an ICP-MS (NexION 2000, PerkinElmer, USA) [16]. The concentrations of As(III) and As(V) were quantified using high-performance liquid chromatography-atomic fluorescence spectroscopy (HPLC-AFS, SA-20, Jitian Inc., China) [11,12]. The speciation of adsorbed As/Fe on the birnessite particles at the end of the incubation period was assessed by XPS (ESCALAB 250Xi, Thermo, USA).

2.4.2. Nitrogen redox transformations

Concentrations of dissolve inorganic N species (NH_4^+-N, NO_3^--N and NO_2^--N) were determined to evaluate the loss/gain of N-derived electron donors/acceptors contributing to As/Fe/Mn redox (bio) transformations [13,27]. Specifically, the salicylate, hydrazine reduction and sulfanilamide/N-1-naphthylethylene spectroscopy methods were applied for quantification of NH_4^+-N, NO_3^--N and NO_2^--N using a continuous-flow analyzer (Autoanalyser-3, Seal, Germany) [28]. N_2O was determined using a gas chromatograph (GC, Agilent 7890, USA) equipped with an electron capture detector. Reactions related to biological N redox transformations incorporating $^{15}N/^{14}N$-labelled components are listed in Table S3. To determine the abundances of $^{30}N_2$, $^{29}N_2$ and $^{28}N_2$ in the N-amended assays, the headspace gas was collected using an aspirator pump to transfer a gas sample from the incubated soil microcosm to a 20-mL pre-evacuated glass vial. All gas samples were sealed with a butyl rubber septum secured by a crimped aluminum closure. The abundances of $^{30}N_2$, $^{29}N_2$ and $^{28}N_2$ in the headspace gas were measured using an isotope ratio mass spectrometer with a ± 0.5‰ precision for $\delta^{15}N$ (IRMS, Thermo Finnigan Delta V Advantage, Germany) [18]. Determination of ^{15}N-nitrate utilized the bacterial denitrifier method [32]. In brief, the denitrifying bacteria *Pseudomonas aureofaciens* (ATCC 13985, USA) transformed nitrate to gaseous nitrous oxide (N_2O) for detection of $^{46}N_2O$ using a continuous-flow isotope ratio mass spectrometer (Delta V, Thermo Fisher Scientific).

2.4.3. Determination of denitrifying enzymes and ETS activities

The activities of denitrifying enzymes play a critical role in regulating N redox transformations. To further assess the impacts of birnessite on denitrification processes, the expressions of four key denitrifying enzymes (NAR (NO_3^-→NO_2^-), NIR (NO_2^-→NO), NOR (NO→N_2O) and NOS (N_2O→N_2)) were determined according to the manufacturer's protocols for the ELISA Kit (Jiangsu Meimian Industrial Co., China) [39]. In this work, activity of the electron transport system (ETS) was determined to reflect the holistic electron transport performance of anaerobic bacteria associated with denitrification [26,51], as assessed by the INT (2-(p-iodophenyl)− 3-(p-nitrophenyl)− 5-phenyltetrazolium chloride) method [47]. Herein, the samples derived from the nitrate alone and combined nitrate-birnessite (0.06 and 0.10 g) treatments incubated for 4 days were collected to determine the activities of ETS and denitrifying enzymes. In brief, 2 g flooded soil, 2 mL Tris-HCl buffer (pH=8.4) and 0.5 mL 0.2% INT solution were mixed in a 10-mL sterilized tube. The mixtures were incubated at 35 °C in a water-bath environment for 30 min in the dark, and then 1 mL formaldehyde (37%) was added to terminate the reaction. The resulting precipitates were collected by centrifugation at 4000 *g* for 5 min and the filtrate discarded. The precipitate was then extracted by mixing with 5 mL methanol and shaken (200 rpm) at 35 °C for 10 min in the dark. The mixture was centrifuged at 4000 *g* for 3 min to measure the volume and absorbance at 485 nm of the supernatant. The INT-ETS activity was calculated according to formula (F1):

$$U = \frac{D_{485} \times V}{K \times w \times t} \quad \text{(F1)}$$

where U is the ETS activity (mg/(mg·h)); D_{485} is the absorbance of the supernatant at 485 nm; V is the volume of the extractant; K is the slope of the standard curve; w is the mass of soil sample; and t is the incubation time.

2.4.4. DNA extraction, library construction, and metagenomic sequencing

Soil samples derived from CK, nitrate, birnessite (0.10 g) and combined nitrate-birnessite (0.10 g) groups were collected after 4 days of incubation for metagenomic sequencing. Total genomic DNA was extracted from 0.5 g soil using duplicate samples (n = 3) from each treatment using the Mag-Bind® Soil DNA Kit (Omega Bio-tek, USA) according to manufacturer's instructions. The concentration and purity of extracted DNA were determined using a NanoDrop2000. The quality and integrity of the DNA extracts was assessed on 1% agarose gel. DNA extract was fragmented to an average size of about 400 bp using Covaris M220 (Gene Company Limited, China) for paired-end library construction. The paired-end library was constructed using NEXTFLEX® Rapid DNA-Seq (Bioo Scientific, USA). Adapters containing the full complement of sequencing primer hybridization sites were ligated to the blunt end of fragments. Paired-end sequencing was performed on Illumina NovaSeq (Illumina Inc., USA) at Majorbio Bio-Pharm Technology (Shanghai, China) using NovaSeq 6000 S4 Reagent Kit v1.5 (300 cycles) according to manufacturer's instructions (www.illumina.com).

Metagenomic data were assembled using MEGAHIT (version 1.1.2). Data were analyzed on the online Majorbio Cloud Platform (www.majorbio.com). Briefly, the paired-end Illumina reads were trimmed of adaptors, and low-quality reads (length <50 bp or with a quality value <20 or having N bases) were removed by fastp (version 0.23.0) [8]. Approximately 13 Gbp (13.03–16.23 Gbp) of clean reads were generated per sample. Filtered metagenomic reads were used for taxonomic classification by kraken2 and bracken against nr-derived databases including Greengenes, SILVA and Ribosomal database project (RDP) [41]. Contigs with lengths over 300 bp were selected as the final assembling result and were subsequently used for further gene prediction and annotation. Functional profiling was performed using Diamond [6] against UniRef90 to obtain gene families (alignment length 25aa, identity 80%, and e-value $1e^{-5}$) [35]. RPKM (Reads Per Kilobase Million) mapped reads were used to estimate genera abundance and gene expression [55]. Gene families were annotated to KEGG Orthogroups, EC categories, eggNOG, Pfam domains and GO terms using Humann's built-in scripts [3]. Detailed information regarding the metagenomic sequencing protocols was provided in Method S2.

2.5. Data analysis

Data were analyzed and visualized using Origin 2024, Microsoft Excel 2016 and SPSS 20.0 software. The standard deviations of triplicate analyses were reported as error bars in the corresponding graphs. Statistical comparisons were determined by analysis of variance using SPSS with a 95% confidence level ($P < 0.05$).

3. Results and discussion

3.1. N redox transformations in flooded paddy soils

Throughout the 8-d incubation period, the NH_4^+-N concentration gradually increased in all amendments (Fig. S2) indicating prominent microbial N mineralization from the background soil. Notably, dissimilatory nitrate reduction to ammonia (DNRA) commonly requires a relatively high C/NO_3^- molar ratio (>12) [36,37]. Thus, the increased NH_4^+ concentration was deemed implausible from DNRA owing to the very low (~1) C/NO_3^- molar ratio. With nitrate amendment, the concentrations of NO_3^--N (Fig. 2a) rapidly decreased and were completely depleted after 4 days, thereby inferring enhanced denitrification and/or NRAO [7]. Notably, the larger dosage of birnessite (0.10 vs. 0.06 g) led to a larger loss of NO_3^--N. On the first day, the 0.10 g birnessite-nitrate treatment induced a greater loss (~60.1%) of NO_3^--N than the 0.06 g birnessite-nitrate (~34.4%) and nitrate alone (~21.4%) treatments. The greater loss of NO_3^--N in the nitrate-birnessite treatment appears to contribute to a greater production of NO_2^- and N_2O through an incomplete denitrification process. However, the dosage-dependent effect of birnessite on suppressing the production of NO_2^--N and N_2O (Fig. 2b-c) in the nitrate-birnessite amendment conflicts with this inference, as the production of NO_2^--N and N_2O derived from the nitrate-birnessite amendment on the second day were decreased by at least 70% and 33%. These contradicting results reveal a mechanism whereby birnessite regulates N redox biotransformation processes by inhibiting the activities of denitrifying enzymes and/or expression of denitrifying genes [13]. Moreover, birnessite is likely to participate in several additional biogeochemical processes in association with redox conversions of NO_3^-/NH_4^+ [14]. These mechanistic inferences are further explored in the following sections (Sections 3.3 and 3.4.2).

3.1.1. Birnessite inhibits N_2O emission through stimulating anammox-related reactions

We found that birnessite amendments diminished the emission of N_2O (Fig. 2c). After incubating for 8 days, the accumulated N_2O was up to 2.4 mM in the nitrate alone treatment versus 0.2–0.3 mM in the nitrate-birnessite amendment. This highlighted that N availability is regulated in part by the presence of birnessite. On the first day, the birnessite treatment (not sealed in dialysis bag) induced a remarkable loss of NH_4^+-N in both the liquid and solid phases in a dose-dependent manner (Fig. 2e). In contrast, no significant loss of NH_4^+-N was found between the CK group and semi-permeable dialysis bag with birnessite assays that isolated the birnessite particles and microbes. This highlights that direct cell-mineral contact contributed to loss of NH_4^+-N in birnessite-supplemented assays. Herein, we preliminarily posit that the loss of NH_4^+-N is related to its participation in anammox/Feammox/Mnammox reactions (Fig. 1b) [13,46].

To validate this hypothesis, we examined the results from the N isotopic fractionation of N-gases and nitrate to identify N dynamics resulting from different conversion pathways. The larger amounts of $^{14}NO_3^-$-N (Fig. 2d) and Mn(II) (Fig. S3) in treatments with greater birnessite dosages on the first day provide strong evidence to support that birnessite and soil-derived $^{14}NH_4^+$-N were utilized as reaction substrates to produce ^{14}N-nitrate by the Mnammox process (Eq. S1). Mnammox-derived nitrate might further be utilized as a substrate for microbial

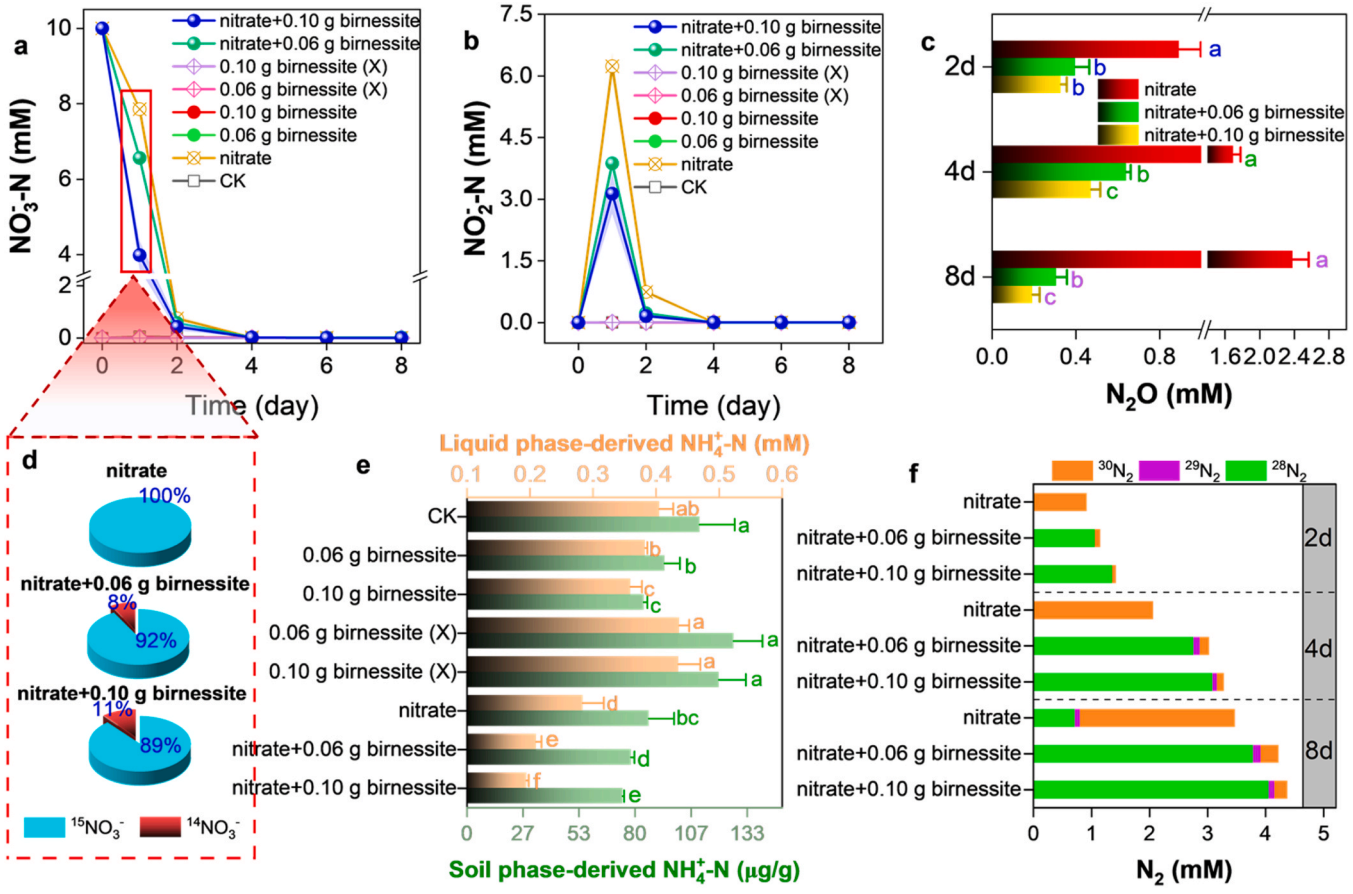

Fig. 2. Nitrate (a) and nitrite (b) concentrations and nitrous oxide emission (c) in flooded paddy soils. The abundances of $^{15}NO_3^-/^{14}NO_3^-$ (d) and corresponding NH_4^+ concentrations in liquid- and soil-phase (e) verify the occurrence of Mnammox/Feammox reactions after incubating for 1 day. The abundances of $^{30}N_2$, $^{30}N_2$ and $^{30}N_2$ trace the pathways of N dynamics in flooded paddy soils. Different lower-case letters on bars indicate significant difference at $P < 0.05$ and the shading indicates the standard error. X represents that the birnessite particles are sealed in a semi-permeable dialysis bag.

As(III) oxidation.

$$NH_4^+ + 4MnO_2 + 6\,H^+ \rightarrow 4Mn^{2+} + NO_3^- + 5\,H_2O \quad (1)$$

Meanwhile, N loss (Fig. 2f) was greatly increased in the nitrate-birnessite amendment. Greater amounts of N_2 (1.4–4.1 mM for 0.10 g and 1.1–3.8 mM for 0.06 g in form of $^{28}N_2$) were emitted from the birnessite-nitrate amendment versus the lower N_2 production (0.9–2.7 mM in form of $^{30}N_2$) observed in the nitrate amendment. Fernandes et al., [17] demonstrated that in a nitrate-limited environment having plentiful ammonia and MnO_x, N_2O was generated through anaerobic nitrification. In contrast, the coexistence of plentiful NO_3^--N, MnO_x, and NH_4^+-N resulted in the predominant generation of N_2 [17]. Although N_2O emission from the birnessite treatment was not measured in this work, our results taken in the context of published research [14, 17] indicates that the combined nitrate-birnessite amendment strengthened anammox/Feammox/Mnammox-derived reactions, thereby attenuating the production of N_2O compared to the nitrate or birnessite treatments. Hence, the above results provide strong evidence that adding birnessite promotes the anaerobic oxidation of ammonia and effectively suppresses N_2O emission from flooded paddy soils having high background ammonia concentrations [14,23].

3.1.2. *Coexistence of nitrate enhanced MnO_2-regeneration and As(III) immobilization*

A greater addition of birnessite induced a larger loss of nitrate rather than producing larger amounts of NO_2^--N and N_2O (Fig. 2b-c). This contradicting phenomenon might be attributed to the nitrate participating in the re-oxidation of Mn(II) (Eq. 2), whereby Mn(II) and nitrate are in turn utilized as the electron donor and acceptor for Mn-oxidizing bacteria [44]. Surplus nitrate in the nitrate-birnessite amendment led to a smaller release of Mn(II) than the birnessite amendment (Fig. S3). The reduced Mn(II) could be regenerated to biogenetic MnO_2 in a catalytic cycle and correspondingly increase the availability of MnO_2, which further favors N transformations and As immobilization in flooded soils. Considering the rank order of oxidation potentials for redox couples (Table S4), thermodynamics preferentially favor MnO_2 reduction, followed by the reduction of nitrate, As(V) and FeO_x [4]. Thus, the redox coupling of nitrate and birnessite ensures the replenishment of MnO_2 and the subsequent oxidation of ammonia to nitrate, nitrite and N_2.

This redox coupling favors the Mnammox reaction that attenuates N_2O emission relative to the Feammox reaction, while also increasing the bioavailability of MnO_2 to induce As(III) immobilization. The release of As in flooded soils is positively correlated with the reductive dissolution of Fe(III)-(oxyhydr)oxides [1]. Hence, the regenerated biogenetic MnO_2 particles can prevent the reductive dissolution of As(V)/Fe(III)-bearing minerals under anoxic conditions. These results provide a key mechanistic insight into how the combined nitrate-birnessite amendment simultaneously suppresses As(III) mobilization and N_2O emission from flooded paddy soils.

$$2NO_3^- + 5Mn^{2+} + 4\,H_2O \rightarrow 5MnO_2 + N_2 + 8\,H^+ \quad (2)$$

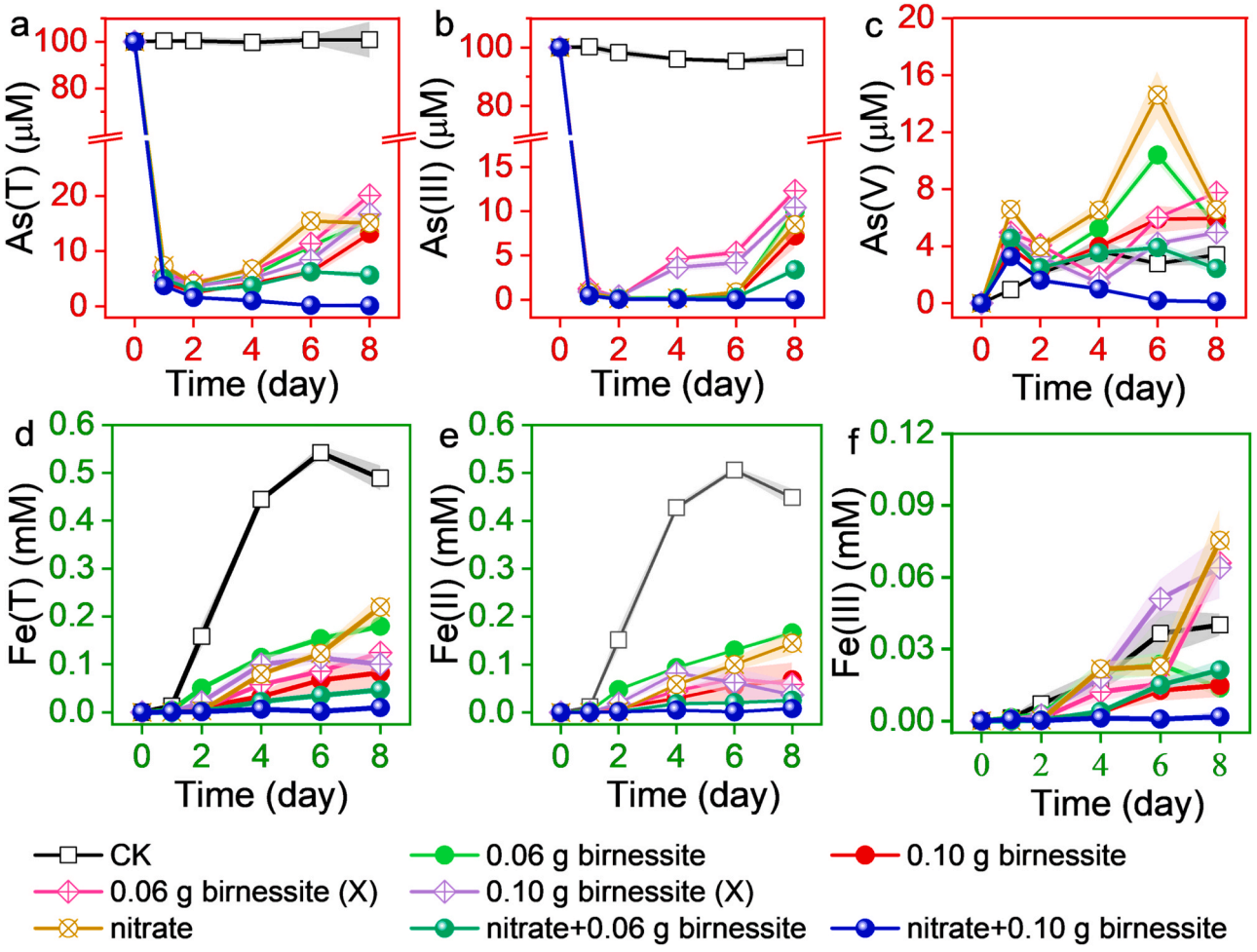

Fig. 3. Concentrations of dissolved As(T) (a), As(III) (b), As(V) (c), dissolved Fe(T) (d), Fe(II) (e) and Fe(III) (f) released in flooded paddy soils throughout the 8-day incubation period (the shading indicates the standard error).

3.2. (Im)mobilization of As/Fe/Mn in flooded paddy soils

3.2.1. Synergetic effects between birnessite and nitrate ensure sustained As/Fe immobilization

Among all treatments, the CK group sustained a favorable metal-reducing condition and fostered the reductive dissolution of As(V)/Fe (III) in the flooded paddy soils (Fig. 3a and Fig. 3d). In the experimental groups, nitrate and birnessite were utilized to boost As(III) oxidation by biotic and abiotic interactions. Based on the dissolved concentrations of As(T), As(III) and As(V) (Figs. 3a-3c), As(III) immobilization was enhanced as the birnessite dosage increased. With the input of nitrate and/or birnessite, dissolved As(T) and As(III) concentrations markedly declined during the initial 2 days of the incubation, suggesting that As (III) immobilization was governed by birnessite oxidation and/or NRAO [49]. After 4 days, a very low level (~1.1 μM) of As(T) was detected from the 0.10 g birnessite-nitrate treatment, whereas there was 3.8 and 7.6 μM of As(T) remaining in the 0.06 g birnessite-nitrate and nitrate treatments. This reveals that As(III) immobilization was effectively achieved by the combined birnessite-nitrate amendment. Since birnessite possesses a considerably high oxidation potential and adsorption capability [49], As(III) and Fe(II) could be efficiently oxidized (reactions of Eq. 3-Eq.7) and adsorbed by birnessite. Subsequently (4–8 days), As (III) concentrations gradually increased and became similar to As(T) concentrations, which was attributed to the consumption of NO_3^--N and/or attainment of As/Fe sorption saturation with birnessite. Following nitrate depletion and saturation of birnessite sorption sites, the redox condition of the microcosm that initially favored As(III) oxidation gradually altered to a condition dominated by dissimilatory metal reducing bacteria that fostered the reductive dissolution of As (V)/Fe(III) [7,10].

$$MnO_2 + H_3AsO_3 + 2\,H^+ \rightarrow Mn^{2+} + H_3AsO_4 + H_2O \quad (3)$$

$$H_2O + 2\,MnO_2 + H_3AsO_3 \rightarrow 2\,MnOOH^* + H_3AsO_4 \quad (4)$$

$$2\,MnOOH^* + H_3AsO_3 + 4\,H^+ \rightarrow 2\,Mn^{2+} + H_3AsO_4 + 3\,H_2O \quad (5)$$

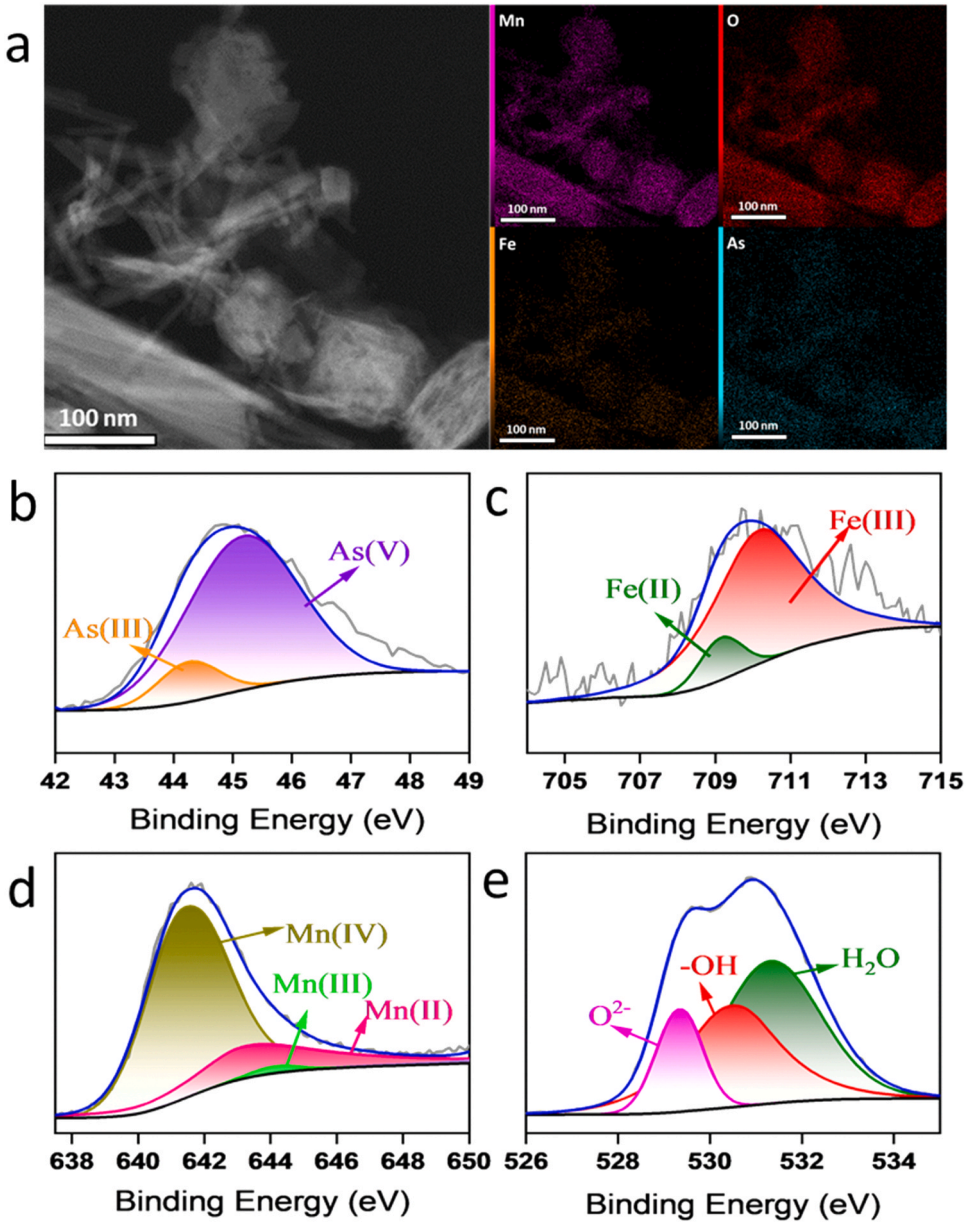

Fig. 4. TEM morphology (a) of birnessite particles and corresponding EDS maps of Mn, Fe, As and O distribution. XPS spectra showing speciation of adsorbed As (b), Fe (c), Mn (d) and O (e) on birnessite particles.

$$2\ \text{Mn-OH} + H_3AsO_3 \rightarrow (MnO)_2AsOOH + 2\ H_2O \quad (6)$$

$$4\ H^+ + 2\ Fe^{2+} + MnO_2 \rightarrow Mn^{2+} + 2\ Fe^{3+} + 2\ H_2O \quad (7)$$

The addition of birnessite and/or nitrate also prominently attenuated the reductive dissolution of Fe(III) in flooded paddy soils (Figs. 3d-3f). Based on the concentrations of released Fe(T) and Fe(II), the overall effects of different amendments on suppressing microbial Fe(III) reductive dissolution followed: 0.10 g birnessite-nitrate > 0.06 g birnessite-nitrate > 0.10 g birnessite > nitrate > 0.06 g birnessite. While no detectable levels of Fe(T) and As(T) were found in the 0.10 g birnessite-nitrate treatment (Fig. 3a and Fig. 3d), considerably higher As (III) concentrations (5.9–19.2 μM) remained in the other treatments at the end of incubation period. This demonstrates that the nitrate or birnessite treatments had a limited impact on As(III) immobilization capacity at the dosages utilized.

As the MnO_2/Mn^{2+} couple has a higher redox potential than the $H_2AsO_4^-/H_3AsO_3$ and Fe^{3+}/Fe^{2+} couples [4], MnO_2 is the most preferentially available electron acceptor to take part in microbially-mediated dissimilatory Mn(IV) reduction via coupling with anaerobic ammonia and/or organic carbon oxidation [14]. Thus, thermodynamic processes are preferentially controlled by Mnammox rather than Feammox and microbial As(V)/Fe(III) reduction, effectively hindering the release of Fe (II) and As(III). Further, TEM and XPS characterization (Figs. 4a-4c) confirmed that MnO_2 was strongly oxidized and adsorb the released Fe (II) and As(III) [29]. Therefore, the suppressed As(III) mobilization resulting from birnessite addition was attributed to the synergistic effects from the coupling of Mn, N, Fe and As biogeochemical cycles, which comprised several concomitant reactions that could lead to As(III) immobilization. Overall, the combined birnessite-nitrate treatment exhibited a strong efficacy for As(III) immobilization at the end of incubation period highlighting its potential as a remediation strategy for dealing with As contaminated paddy soils.

3.2.2. *Chemical and biological coupling between nitrate, birnessite and microbes*

In the combined nitrate-birnessite treatment, birnessite-induced abiotic As(III) oxidation occurs preferential to microbial As(III) oxidation, because the $MnO_2/Mn(II)$ couple has a higher redox potential than the NO_3^-/NO_2^- couple (0.57 V vs. 0.43 V; Table S4) [4]. That is why we observed higher Mn(II) release in the birnessite treatment (not sealed in the semi-permeable dialysis bag) on the first day (Fig. S3). To identify the existence and speciation of As and Fe adsorbed onto birnessite particles, we isolated the birnessite particles in the dialysis bag for TEM inspection and XPS analysis. TEM-EDS mapping provided direct evidence for the sorption of As and Fe on birnessite surfaces (Fig. 4a). The content and valence of adsorbed As and Fe were further assessed by XPS. The larger integral areas for the fitted peak of As(V) than As(III) (45.7 versus 44.8 eV in the As 3d spectrum) and Fe(III) than Fe(II) (709.0 versus 710.8 eV in the Fe 2p spectrum) indicated a dominance of As(V) (87.6%) and Fe(III) (88.4%) on the birnessite surface (Figs. 4b-4c and Table S5). The representative peaks for Mn(II) and Mn(III) with binding energies located at 644.2 and 643.1 eV are presented in the Mn 2p spectrum (Fig. 4d) [16]. The results indicated that Mn(III) species were produced during the redox reactions with Mn(IV)/Mn(II). Three overlapping peaks assigned to the functional groups of lattice oxygen (O^{2-}), hydroxyl (-OH) and adsorbed water (H_2O) (529.60, 531.72 and 532.84 eV) were identified in the O 1 s spectrum (Fig. 4e). The relatively high O^{2-} and -OH group contents (15.8% and 35.5%) in oxygen-bearing groups (Table S5) provide evidence for the existence of active surface sites available for adsorption and/or complexation with released Mn(II) and As(V)/Fe(III).

The progressive release of NH_4^+ from the flooded paddy soils (Fig. S2) provides a critical substrate to support the activities of Feammox bacteria. This implies that the reductive dissolution of Fe(III)-bearing minerals with a concomitant release of As might occur when nitrate is depleted. The limited release of As/Fe highlights that the combined birnessite-nitrate treatment achieved a prominent and durable As(III)-immobilization effect even under conditions favorable for the dissolution of Fe(III)/As(V). This paradox results from the continuous redox recycling that is coupled to simultaneous Feammox/Mnammox and denitrification that maintains the redox potential in favor of As(III)-immobilization. In flooded NH_4^+/Fe/Mn-rich paddy soils, biological ammonia oxidation (to either nitrate, nitrite or N_2) is facilitated by FeO_x/MnO_x serving as terminal electron acceptors [14]. The subsequent denitrification of these product (NO_2^-/NO_3^-) could be linked to the oxidation of reduced FeO_x/MnO_x, which enables the recycling of FeO_x/MnO_x and provides renewed oxide surfaces to support the next cycle of Feammox/Mnammox. Therein, the surplus nitrate is important for sustaining a reliable recycling and catalytic effect of the regenerated MnO_2.

Treatment with birnessite or nitrate alone exhibited inferior As(III) immobilization effects, as birnessite-induced As(III) adsorption was nearly saturated by the 2nd day (confirmed from the sealed assays in Fig. 3b) and nitrate was nearly depleted on the 4th day in all nitrate-supplemented assays (Fig. 2a). This implies that As(III) immobilization is difficult to achieve through birnessite-induced adsorption/oxidation or microbially driven NDAO processes during the subsequent 4–8 days of incubation. In contrast, we found virtually no As(III) was released from the combined birnessite-nitrate assays during the subsequent 4–8 day period. We also found that birnessite addition without sealing in a dialysis bag (i.e., direct birnessite-microbial cell contact) achieved a better As(III) immobilization effect than the birnessite treatment within the dialysis bag (i.e., no direct contact between microbial cells and birnessite). This difference is ascribed to microbially-driven denitrification and Feammox/Mnammox leading to the generation of reactive N species as intermediate products of metabolism (NO_3^- and NO_2^-, shown in Eq. S4-S6 in Table S3). These intermediate N products in turn react with Mn^{2+} to produce biogenetic MnO_2 through a side reaction of denitrification catalyzed by heterotrophic bacteria using organic carbon [21,40]. As a result, the nitrate containing nitrate-birnessite treatment (versus no nitrate in the birnessite treatment) was more conducive to the regeneration of biogenetic MnO_2. This explains why the combined nitrate-birnessite treatment sustained satisfactory As(III) immobilization capacity through the entire incubation period. Hence, these findings document an integrated chemical-biological reaction series governed by a birnessite-nitrate-microbe alliance that controls As(III) mobilization and N redox transformations.

3.3. *Suppressed denitrification ETS activity and denitrifying enzymes activities in response to birnessite amendment*

Microbial denitrification requires effective transport and consumption of electrons in an enzymatic complex called the microbial ETS (Fig. 5a) [34,54]. The birnessite treatment displayed an obvious dosage-dependent-inhibition effect on ETS activity (declined by 10–15%) (Fig. 5b). The suppression effect was attributed to the MnO_2/Mn^{2+} couple that has a higher redox potential than the NO_3^-/NO_2^- couple. This ensures a larger electron consumption by MnO_2 reduction as opposed to nitrate reduction (i.e., denitrification process) [4], which leads to a decline in the related denitrification ETS activities in the birnessite-amended assays. In microbial denitrification ETS, electrons produced by microbial metabolism are consumed by four functional denitrifying enzymes (NAR, NIR, NOR and NOS) that are in turn responsible for each step of the denitrification process ($NO_3^- \rightarrow NO_2^- \rightarrow NO \rightarrow N_2O \rightarrow N_2$) [34]. In contrast, higher activities of denitrifying enzymes were found in nitrate-amended assays (Fig. 5c) as the abundance of nitrate stimulates the activities of denitrifying enzymes. Consistent with the ETS performance, birnessite induced a prominent dosage-dependent suppression on the activities of denitrifying enzymes. These inhibited activities demonstrated that birnessite attenuates the electron consumption capabilities of the denitrifying enzymes through inhibition of ETS activity that hinders the electron flux

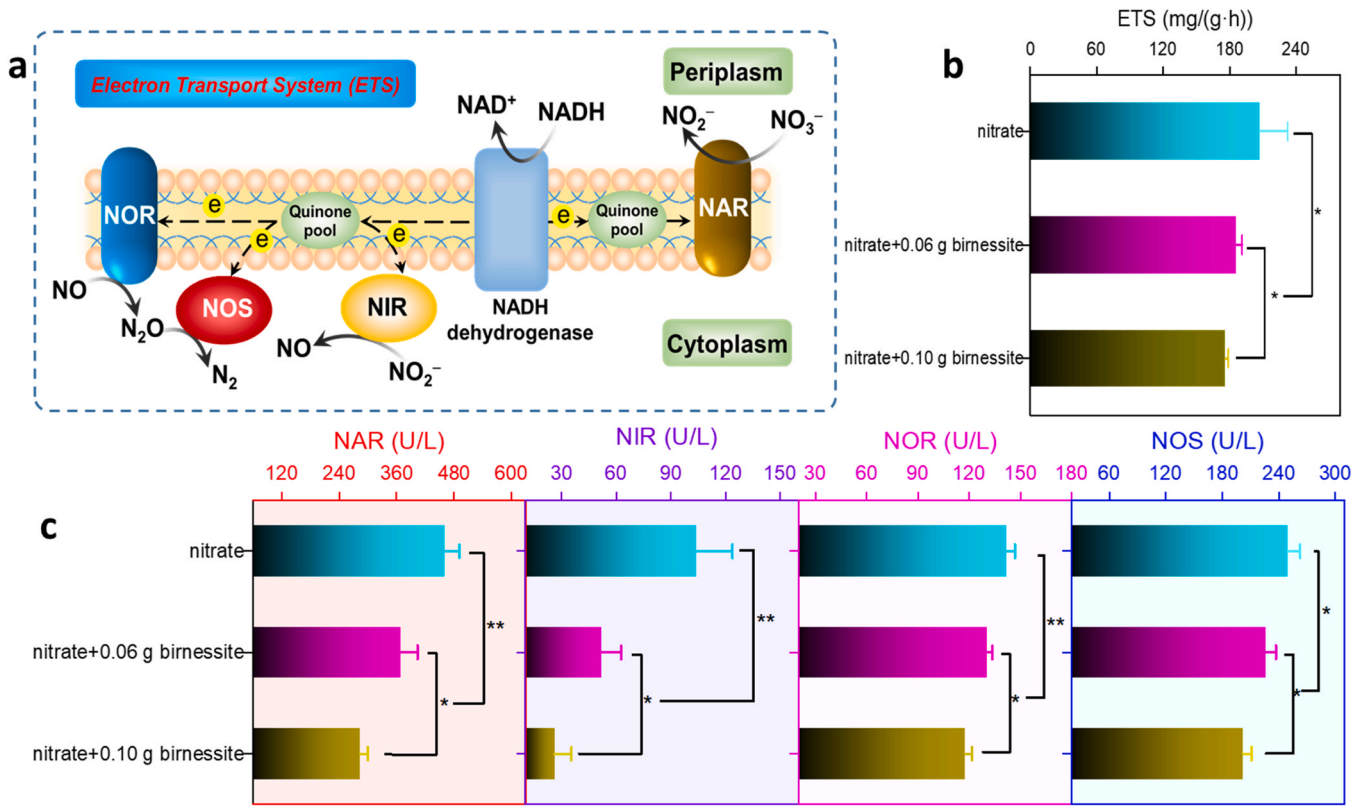

Fig. 5. Schematic diagram of electron transport mediated by denitrifying enzymes in the denitrification ETS (a). The activities of ETS (b) and denitrifying enzymes (c) in response to the addition of nitrate and/or birnessite.

to drive denitrification. Correspondingly, the inhibitory effect inevitably causes poor electron transport efficiency that hinders the low production of NO_2^--N and N_2O in the combined birnessite-nitrate treatment (Fig. 2b-c). The reduced activities of ETS and the underlying catalytic activities of denitrifying enzymes result in sluggish electron transfer and elevated NO_3^- and/or NO_2^- levels in the nitrate-birnessite treatment. The surplus NO_3^--N and NO_2^--N is then available to participate in microbial nitrate-dependent Mn(II)/Fe(II) oxidation (Eqs. S11-S15 in Table S3). Thus, modulation of denitrification ETS with the coexistence of birnessite and nitrate is conducive to the regeneration of FeO_x/MnO_x.

3.4. Bacterial taxonomic composition and potential functions

3.4.1. Shift in the composition of bacterial communities

Metagenomic sequencing indicated that Proteobacteria (27–32%) and Actinobacteria (21–30%) were dominant in the microbial community at the phylum level, followed by Chloroflexi (6–8%) and Planctomycetota (4–7%) (Fig. 6a). Compared to the CK group, nitrate and birnessite amendments led to a remarkable enrichment of Proteobacteria and decrease of Actinobacteria. The changes in bacterial communities responding to the addition of nitrate and/or birnessite were further evaluated by principal coordinate analysis (PcoA) based on the weighted Fast UniFrac metric (Fig. 6b). Principal axis 1 explained 89.4% of the variability among samples. The overlapping area between the two treatments revealed a close similarity in microbial communities. Therein, the larger overlap between the combined nitrate-birnessite treatment with the nitrate treatment versus the birnessite treatment demonstrates that nitrate was a more important driver than birnessite in shaping the bacterial community of the combined nitrate-birnessite treatment. The bubble plot of RPKM abundances for genera confirmed that the representative Fe(III)/As(V)-reducing bacteria (e.g., *Geobacter*, *Bacillus* and *Desulfuromonas*) were the most dominant genera in the CK group (Fig. 6c). These enriched bacteria are presumed to be responsible for the reductive dissolution of Fe(III)/As(V) in flooded paddy soils. When deprived of nitrate, these bacteria obtain energy for anoxic growth through coupling dissimilatory metal reduction with acetate/ammonia oxidation [10,43].

The addition of nitrate induced a decrease in the abundance of As (V)/Fe(III)-reducing genera and an increase in the abundance of As (III)/Fe(II)/Mn(II)-oxidizing genera. The abundances of metal-oxidizing genera (e.g., *Azoarcus*, *Streptomyces*, *Methylobacterium*, *Marinobacter daepoensis* and *Cupriavidus*) were markedly increased in birnessite and/or nitrate treatments. Notably, versatile genera, such as *Pseudomonas*, *Achromobacter* and *Cupriavidus*, are capable of oxidizing As(III)/Fe(II)/Mn(II) by utilizing nitrate or nitrite as electron donors and were highly enriched in the combined birnessite-nitrate treatment [2,24,33]. The birnessite-nitrate amendment provides a flexible strategy for shifting the microbial community composition of flooded paddy soils. The enrichment of metal-oxidizing microbes in birnessite-nitrate treatments opens more possibilities for synergetic associations between NO_3^-/NO_2^- and Fe(II)/Mn(II) transforming bacteria, thereby foster the regenerative/recycling of Fe(III)/Mn(IV).

3.4.2. Changes in the abundance of functional genes

To explore the potential functions of microbial communities, key functional genes involving As, Fe, Mn and N metabolic processes were annotated by the KEGG Orthologs database. The functions and RPKM abundances of key genes responsible for As/Fe/Mn/N cycling are summarized/visualized in Table S6/Fig. S4. Since most microbes harbor the capability for As detoxification metabolism [50], the As-transporting genes (*arsB* and *arsA*) and As(V)-reducing genes (*arsC* and *arsR*) were dominant across all amendments (Fig. S4). A heat map (Fig. 7) revealed that the addition of nitrate markedly increased the abundance of As (III)-oxidizing genes (*aoxA* and *aoxB*). Bacteria carrying Mn (II)-oxidizing genes are a prerequisite for replenishing biogenetic MnO_2 [40]. As expected, additions of nitrate and birnessite increased the

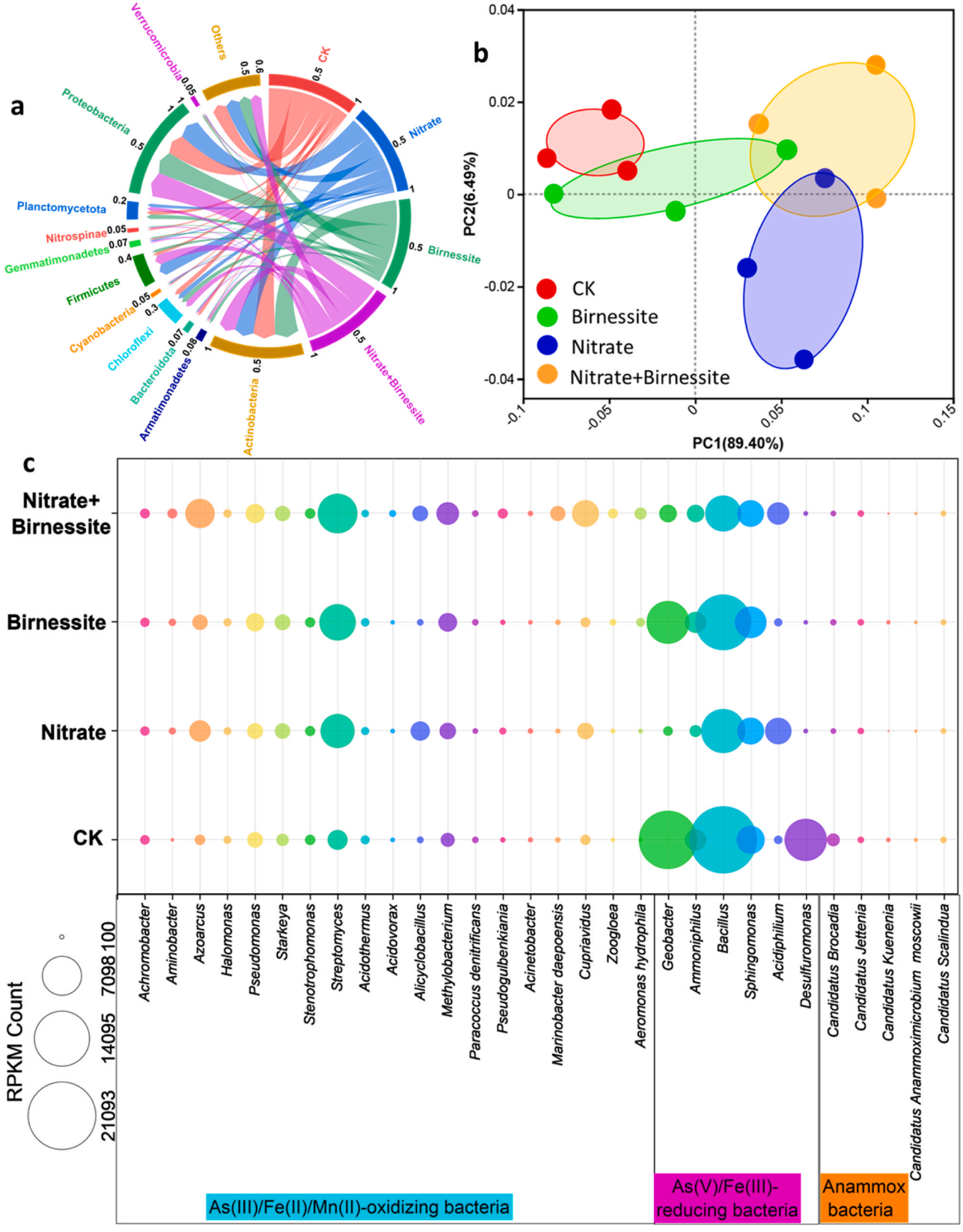

Fig. 6. The distribution of microbial community at phylum level (a), PCoA of microbial diversity based on Operational Taxonomic Units using the weighted Fast UniFrac metric (b), and the RPKM (Reads Per Kilobase Million) abundances of key genera responsible for the biotransformation of As/Fe/Mn/N under different amendments. Dosages in the birnessite alone and birnessite-nitrate treatments are both 0.10 g.

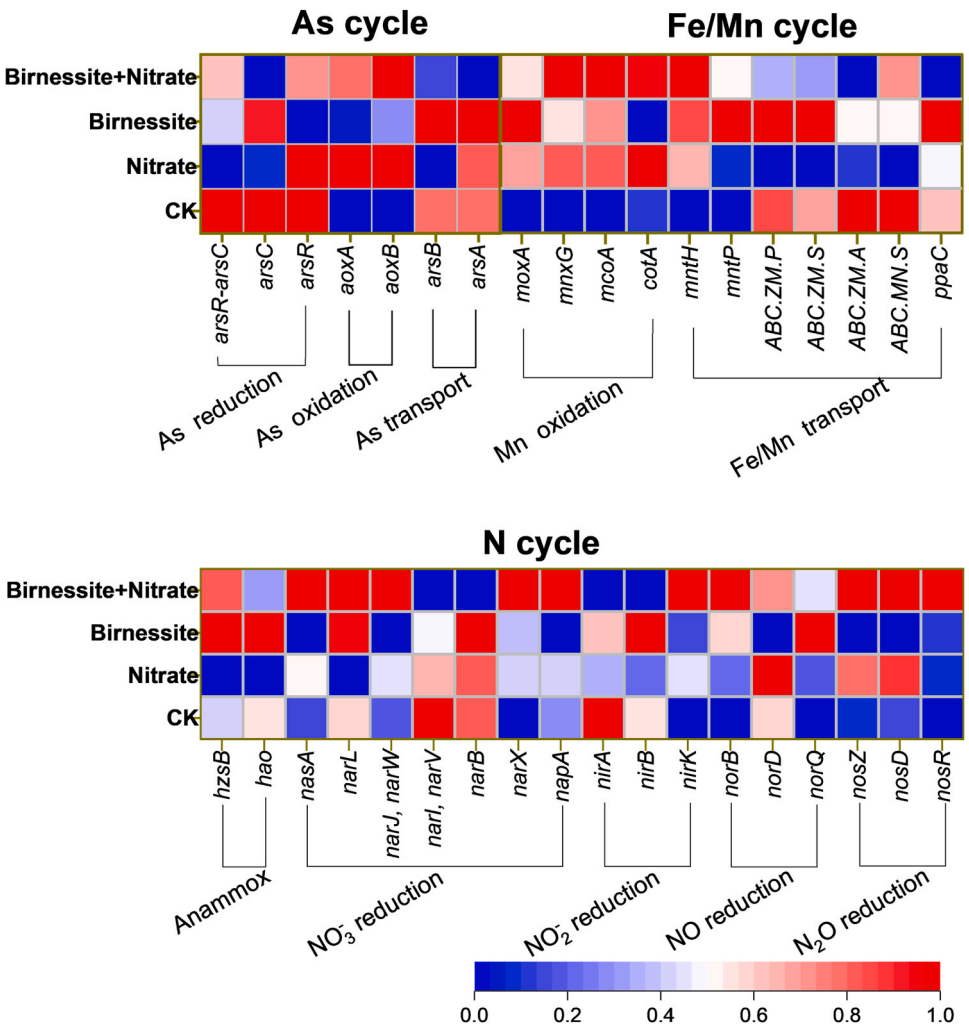

Fig. 7. Heat map of relative abundances of key functional genes responsible for biotransformation of As/Fe/Mn/N under different amendments. Dosages in the birnessite alone and birnessite-nitrate treatments are both 0.10 g.

abundances of Mn(II)-oxidizing genes (*moxA*, *mnxG*, *mcoA* and *cotA*). Hence, the nitrate-birnessite amendment promotes a facile bacterial strategy to acquire and maintain biogenetic MnO_2, that in turn suppresses As(III) mobilization and denitrification.

The nitrate and birnessite treatments displayed contrary results with respect to the abundances of N cycle-related genes (anammox vs. denitrification). For instance, the nitrate treatment increased the abundances of several denitrifying genes (*nasA*, *narJ*, *narW*, *nirK*, *norD*, *nosZ* and *nosD*), whereas the birnessite treatment increased the abundance of anammox-related genes (*hzsB* and *hao*) compared to the CK group. The difference in the abundance of N cycle-related genes between the nitrate and birnessite treatments implies a unique microbial evolution strategy to modulate contrasting N metabolic pathways. Notably, the abundances of nitrate-reducing genes (*nasA*, *narL* and *narJ, narW*), nitrite-reducing gene (*nirK*), NO-reducing gene (*norD*) and N_2O-reducing genes (*nosZ*, *nosD* and *nosR*) represented a considerably high proportion of all denitrifying genes (Fig. S4) and their abundances were higher in the combined nitrate-birnessite versus nitrate treatment (Fig. 7). However, this increased abundance of denitrifying genes was not consistent with the suppressed denitrification found in the combined nitrate-birnessite treatment (Fig. 2b-c). Pearson correlation analysis (Fig. S5) indicated that the activities of denitrifying enzymes were a crucial factor associated with the production of nitrite and N_2O, whereas the transcript levels of denitrifying genes shows no significance differences with respect to the production of NO_2^--N and N_2O. Thus, the suppressed denitrification in the combined nitrate-birnessite treatment was more strongly associated with the activities of denitrifying enzymes (gene expression level) rather than denitrifying genes (gene level).

3.5. *Mechanisms involving the simultaneous suppression of As mobilization and N_2O emission*

We examined the suppression of As(III) mobilization and N_2O emission by the treatments with nitrate, birnessite and combined birnessite-nitrate (Fig. 8a-c). For the nitrate treatment (Fig. 8a), As(T) immobilization was only effective for the initial 2 days of the incubation while emitting a large amount of N_2O (increased by 1.2–1.7 times vs. nitrate-birnessite treatment). Following nitrate depletion, As(III)-immobilization effectiveness gradually decreased. The attenuated effect was ascribed to the surplus NH_4^+-N derived from the background soil that promoted microbial reductive dissolution of Fe(III) with a concomitant release of As via Feammox [43]. Although the birnessite treatment (Fig. 8b) exhibited strong oxidation/adsorption of As(III), the surplus NH_4^+-N and Feammox-derived Fe(II) in NH_4^+/As-rich paddy soils competed with As(III) for the birnessite-induced oxidation [14]. This infers an inefficient As(III)-oxidation/adsorption due to limited direct As (III)-birnessite interaction. As a result, the anticipated As(III) immobilization effect was greatly diminished for low dosages of birnessite. Overall, neither nitrate or birnessite amendment achieved a satisfactory performance for suppression of As(III) mobilization and N_2O emission in

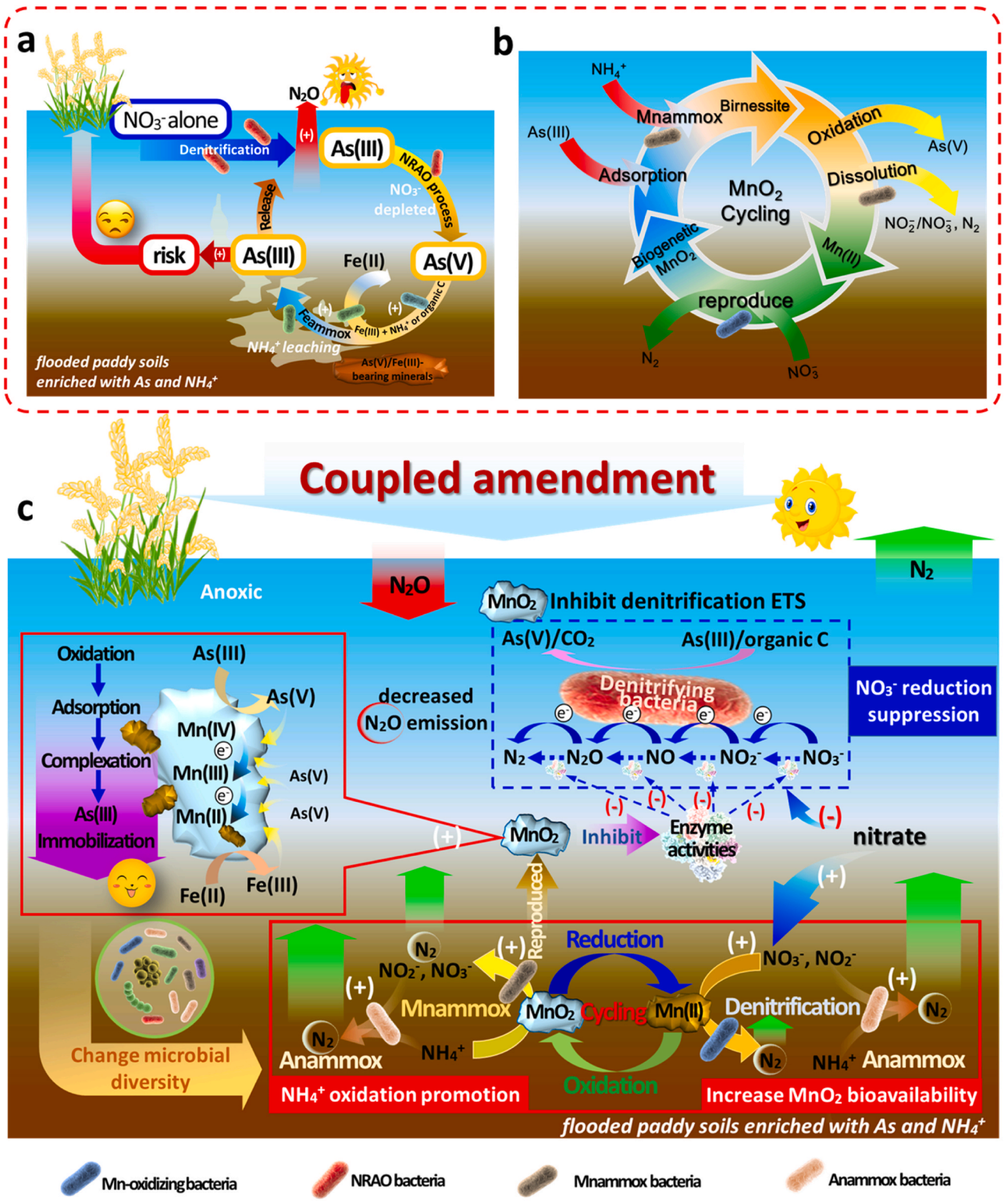

Fig. 8. Schematic representation of response mechanisms for As/Fe/N cycling behaviors to treatment with nitrate (a), birnessite (b) and a combined birnessite-nitrate treatment (c).

flooded paddy soils enriched with NH_4^+ and As(III).

The combined birnessite-nitrate treatment achieved an effective management strategy for simultaneously suppressing As(III) mobilization and N_2O emission (Fig. 8c). Therein, a suitable dosage of nitrate supplies an essential substrate for the enrichment of nitrate-dependent Mn(II)-oxidizing bacteria (e.g., *Pseudomonas*, *Achromobacter* and *Cupriavidus*). These bacteria are capable of oxidizing Mn(II) resulting from Mnammox and/or abiotic As(III) oxidation processes. This is of crucial importance to ensure the successive regeneration/recycling of MnO_2. Moreover, as the activities of enzymes in the denitrification ETS were inhibited by MnO_2, a large amount of nitrate became available for biological oxidation of Mn(II). As a result, the nitrate was consumed by biological Mn(II) oxidation to generate biogenetic MnO_2 (Eq. S14 and Eq.S15) rather than denitrification (Eq. S9, Eq. S12 and Eq. S17), which

effectively diminished N_2O emission. The regenerated biogenetic MnO_2 continues to induce a simultaneous suppression of As(III) mobilization and N_2O emission through recycling, even though nitrate was completely depleted and NH_4^+ was continuously leached after 4 days of incubation. The coupling of birnessite and nitrate by biogeochemical cycling further induced an alternative pathway in the conventional N cycle whereby surplus NH_4^+-N and NO_2^--N were utilized in the anammox process that could effectively circumvent the generation of N_2O [46,48]. Thus, a sufficient supply of available nitrate enables the replenishments of MnO_2 particles that increases the sustained bioavailability of MnO_2 for the effective suppression of As(III) mobilization and N_2O emission.

In the coupled birnessite-nitrate treatment, biological and chemical interactions are synergistically developed through fully utilizing endogenous and exogenous energy sources to improve survival strategies and environmental adaptability of key microbes in paddy soils [52]. These attributes of the combined treatment create synergist potentials for restraining As(III) mobilization and N_2O emission as each component (nitrate and birnessite) contributes its respective advantages while offsetting their corresponding shortcomings. Implementing the combined birnessite-nitrate at the field scale is economically practical as Mn oxides and nitrate are commercially available at a reasonable cost. The next step is to apply the combined birnessite-nitrate treatment at the field scale to confirm its effectiveness and examine its long-term performance in a real-world setting. Overall, this work provides proof-of-concept for a novel approach to replace existing inefficient, conventional remediation strategies with a cost-effective, innovative and sustainable technology for suppressing anoxic As mobilization and N_2O emission in paddy soils.

4. Conclusions

Previous As(III) immobilization studies utilizing nitrate or birnessite amendments in flooded paddy soils experienced several shortcomings, such as elevated N_2O emission, inefficient As(III) immobilization, and a short-term, non-sustainable performance. By contrast, combined birnessite-nitrate amendment achieved virtually no As(T) release and at least a 87% reduction in N_2O compared to a sole nitrate treatment. The combined nitrate-birnessite treatment produced a synergetic association with nitrate contributing to the regeneration of MnO_2 via coupling the biogeochemical cycles of Mnammox and Mn(II)-derived denitrification under a NH_4^+-enriched environment with the coexistence of MnO_2. Due to the suppressed activities of enzymes in the denitrification ETS, the elevated concentrations of nitrate preferentially participated in biological oxidation of Mn(II) rather than denitrification, leading to the regeneration of MnO_2 rather than producing N_2O. With the successive regeneration and recycling of biogenetic MnO_2, effective As(III) immobilization and suppression of N_2O emission were achieved. This study demonstrates the efficacy for the simultaneous mitigation of As(III) mobilization and N_2O emission by a combined nitrate-birnessite treatment in flooded paddy soils enriched in As and NH_4^+.

Environmental Implication

Although microbially-mediated nitrate reducing-As(III) oxidation shows a satisfactory effect on limiting As(III) mobilization, enhanced denitrification generates emission of the greenhouse gas N2O, thereby deterring its practical application. The present study demonstrates that a combined nitrate-birnessite treatment can simultaneously mitigate As (III) mobilization and N2O emission from flooded paddy soils as compared to amending with nitrate or birnessite alone. Therein, nitrate facilitates the regeneration of MnO2, which directly suppresses As(III) mobilization and N2O emission from flooded paddy soils.

CRediT authorship contribution statement

Zhang Jing: Investigation, Writing – original draft. **Hu Jiehua:** Conceptualization, Funding acquisition, Methodology. **Wang Feng:** Conceptualization, Writing – original draft. **Gao Hui:** Conceptualization, Funding acquisition. **Huang Peng:** Investigation. **Chen Zheng:** Funding acquisition, Supervision, Writing – review & editing. **Dahlgren Randy A.:** Writing – review & editing. **Wang Yanhong:** Investigation. **Deng Huanhuan:** Formal analysis. **Wang Honghui:** Conceptualization, Investigation. **Zeng Yanqiong:** Methodology, Software.

Declaration of Competing Interest

The authors declare that they have no known competing financial interests or personal relationships that could have appeared to influence the work reported in this paper.

Data Availability

Data will be made available on request.

Acknowledgments

This work was supported by the National Natural Science Foundation of China (41807035 and 42177066), the Key R&D Plan of Ningxia Hui Autonomous Region (2021BEB04050), the Science and Technology Bureau of Wenzhou, China (N2023011), Natural Scientific Foundation of Fujian Province (2022J01391) and Zhejiang Province Public Welfare Technology Application Research Project (LGF22E080002).

Appendix A. Supporting information

Supplementary data associated with this article can be found in the online version at doi:10.1016/j.jhazmat.2024.133451.

References

[1] Aftabtalab, A., Rinklebe, J., Shaheen, S.M., Niazi, N.K., Moreno-Jiménez, E., Schaller, J., et al., 2022. Review on the interactions of arsenic, iron (oxy)(hydr) oxides, and dissolved organic matter in soils, sediments, and groundwater in a ternary system. Chemosphere 286, 131790.
[2] Bai, Y., Su, J., Wen, Q., Huang, T., Chang, Q., Ali, A., 2021. Characterization and mechanism of Mn(II)-based mixotrophic denitrifying bacterium (*Cupriavidus* sp. HY129) in remediation of nitrate (NO_3^--N) and manganese (Mn(II)) contaminated groundwater. J Hazard Mater 408, 124414.
[3] Beghini, F., McIver, L.J., Blanco-Míguez, A., Dubois, L., Asnicar, F., Maharjan, S., et al., 2021. Integrating taxonomic, functional, and strain-level profiling of diverse microbial communities with bioBakery 3. Elife 10, 65088.
[4] Borch, T., Kretzschmar, R., Kappler, A., Cappellen, P.V., Ginder-Vogel, M., Voegelin, A., et al., 2010. Biogeochemical redox processes and their impact on contaminant dynamics. Environ Sci Technol 44, 15–23.
[5] Boumaiza, H., Coustel, R., Medjahdi, G., Ruby, C., Bergaoui, L., 2017. Conditions for the formation of pure birnessite during the oxidation of Mn(II) cations in aqueous alkaline medium. J Solid State Chem 248, 18–25.
[6] Buchfink, B., Reuter, K., Drost, H.G., 2021. Sensitive protein alignments at tree-of-life scale using DIAMOND. Nat Methods 18, 366–368.
[7] Chen, G., Du, Y., Fang, L., Wang, X., Liu, C., Yu, H., et al., 2023. Distinct arsenic uptake feature in rice reveals the importance of N fertilization strategies. Sci Total Environ 854, 158801.
[8] Chen, S., Zhou, Y., Chen, Y., Gu, J., 2018. Fastp: an ultra-fast all-in-one FASTQ preprocessor. Bioinformatics 34, 884–890.
[9] Chen, Z., Dong, G., Chen, Y., Wang, H., Liu, S., Chen, Z., et al., 2019. Impacts of enhanced microbial-photoreductive and suppressed dark microbial reductive dissolution on the mobility of As and Fe in flooded tailing soils with zinc sulfide. Chem Eng J 372, 118–128.
[10] Chen, Z., Li, H., Ma, W., Fu, D., Han, K., Wang, H., et al., 2018. Addition of graphene sheets enhances reductive dissolution of arsenic and iron from arsenic contaminated soil. Land Degrad Dev 29, 572–584.
[11] Chen, Z., Liu, Y., Zhang, C., Pan, Y., Han, R., Chen, Y., et al., 2019. Titanium dioxide nanoparticles induced an enhanced and intimately coupled photoelectrochemical-microbial reductive dissolution of As(V) and Fe(III) in flooded arsenic-enriched soils. ACS Sustain Chem Eng 7, 13236–13246.
[12] Chen, Z., Wang, Y., Jiang, X., Fu, D., Xia, D., Wang, H., et al., 2017. Dual roles of AQDS as electron shuttles for microbes and dissolved organic matter involved in arsenic and iron mobilization in the arsenic-rich sediment. Sci Total Environ 574, 1684–1694.
[13] Cheng, C., He, Q., Zhang, J., Chai, H., Yang, Y., Pavlostathis, S.G., et al., 2022. New insight into ammonium oxidation processes and mechanisms mediated by manganese oxide in constructed wetlands. Water Res 215, 118251.

[14] Desireddy, S., Pothanamkandathil Chacko, S., 2021. A review on metal oxide (FeO_x/MnO_x) mediated nitrogen removal processes and its application in wastewater treatment. Rev Environ Sci Biotechnol 20, 697–728.
[15] Dong, G., Chen, Y., Yan, Z., Zhang, J., Ji, X., Wang, H., et al., 2020. Recent advances in the roles of minerals for enhanced microbial extracellular electron transfer. Renew Sust Energ Rev 134, 110404.
[16] Dong, G., Han, R., Pan, Y., Zhang, C., Liu, Y., Wang, H., et al., 2021. Role of MnO_2 in controlling iron and arsenic mobilization from illuminated flooded arsenic-enriched soils. J Hazard Mater 401, 123362.
[17] Fernandes, S.O., Javanaud, C., Aigle, A., Michotey, V.D., Guasco, S., Deborde, J., et al., 2015. Anaerobic nitrification-denitrification mediated by Mn-oxides in meso-tidal sediments: Implications for N_2 and N_2O production. J Mar Syst 144, 1–8.
[18] Fuchslueger, L., Wild, B., Mooshammer, M., Takriti, M., Kienzl, S., Knoltsch, A., et al., 2019. Microbial carbon and nitrogen cycling responses to drought and temperature in differently managed mountain grasslands. Soil Biol Biochem 135, 144–153.
[19] Hassouna, M.E.M., Elsuccary, S.A.A., 2002. Determination of oxalate based on its enhancing effect on the oxidation of Mn(II) by periodate. Talanta 56, 193–202.
[20] Islam, S.F.U., de Neergaard, A., Sander, B.O., Jensen, L.S., Wassmann, R., van Groenigen, J.W., 2020. Reducing greenhouse gas emissions and grain arsenic and lead levels without compromising yield in organically produced rice. Agr Ecosyst Environ 295, 106922.
[21] LaRowe, D.E., Carlson, H.K., Amend, J.P., 2021. The energetic potential for undiscovered manganese metabolisms in nature. Front Microbiol 12, 1–16.
[22] Li, H., Santos, F., Butler, K., Herndon, E., 2021. A critical review on the multiple roles of manganese in stabilizing and destabilizing soil organic matter. Environ Sci Technol 55, 12136–12152.
[23] Li, L., Ling, Y., Wang, H., Chu, Z., Yan, G., Li, Z., et al., 2020. N_2O emission in partial nitritation-anammox process. Chin Chem Lett 31, 28–38.
[24] Li, X., Qiao, J., Li, S., Haggblom, M.M., Li, F., Hu, M., 2020. Bacterial communities and functional genes stimulated during anaerobic arsenite oxidation and nitrate reduction in a paddy soil. Environ Sci Technol 54, 2172–2181.
[25] Li, Y., Liu, Y., Feng, L., Zhang, L., 2023. A review: Manganese-driven bioprocess for simultaneous removal of nitrogen and organic contaminants from polluted waters. Chemosphere 314, 137655.
[26] Liu, S., Wang, C., Hou, J., Wang, P., Miao, L., 2020. Effects of Ag NPs on denitrification in suspended sediments via inhibiting microbial electron behaviors. Water Res 171, 115436.
[27] Liu, T., Chen, D., Luo, X., Li, X., Li, F., 2019. Microbially mediated nitrate-reducing Fe(II) oxidation: Quantification of chemodenitrification and biological reactions. Geochim Cosmochim Ac 256, 97–115.
[28] Liu, X., Wu, Y., Sun, R., Hu, S., Qiao, Z., Wang, S., et al., 2020. NH_4^+-N/NO_3^--N ratio controlling nitrogen transformation accompanied with NO_2^--N accumulation in the oxic-anoxic transition zone. Environ Res 189, 109962.
[29] Ma, L., Cai, D., Tu, S., 2020. Arsenite simultaneous sorption and oxidation by natural ferruginous manganese ores with various ratios of Mn/Fe. Chem Eng J 382, 123040.
[30] Nadeau, S.A., Roco, C.A., Debenport, S.J., Anderson, T.R., Hofmeister, K.L., Walter, M.T., et al., 2019. Metagenomic analysis reveals distinct patterns of denitrification gene abundance across soil moisture, nitrate gradients. Environ Microbiol 21, 1255–1266.
[31] Rokonuzzaman, M.D., Li, W.C., Wu, C., Ye, Z.H., 2022. Human health impact due to arsenic contaminated rice and vegetables consumption in naturally arsenic endemic regions. Environ Pollut 308, 119712.
[32] Søvik, A.K., Mørkved, P.T., 2008. Use of stable nitrogen isotope fractionation to estimate denitrification in small constructed wetlands treating agricultural runoff. Sci Total Environ 392, 157–165.
[33] Su, J., Liang, D., Lian, T., 2018. Comparison of denitrification performance by bacterium *Achromobacter* sp. A14 under different electron donor conditions. Chem Eng J 333, 320–326.
[34] Su, X., Chen, Y., Wang, Y., Yang, X., He, Q., 2019. Impacts of chlorothalonil on denitrification and N_2O emission in riparian sediments: Microbial metabolism mechanism. Water Res 148, 188–197.
[35] Suzek, B.E., Wang, Y., Huang, H., McGarvey, P.B., Wu, C.H., Consortium, U., 2015. UniRef clusters: A comprehensive and scalable alternative for improving sequence similarity searches. Bioinformatics 31, 926–932.
[36] van den Berg, E.M., Boleij, M., Kuenen, J.G., Kleerebezem, R., van Loosdrecht, M.C. M., 2016. DNRA and denitrification coexist over a broad range of acetate/N-NO_3^- ratios, in a chemostat enrichment culture. Front Microbiol 7, 1842–1853.
[37] van den Berg, E.M., Elisário, M.P., Kuenen, J.G., Kleerebezem, R., van Loosdrecht, M.C.M., 2017. Fermentative bacteria influence the competition between denitrifiers and DNRA bacteria. Front Microbiol 8, 1684–1696.
[38] Wang, F., Zhang, J., Zeng, Y., Wang, H., Zhao, X., Chen, Y., et al., 2023. Arsenic mobilization and nitrous oxide emission modulation by different nitrogen management strategies in flooded ammonia-enriched paddy soils. Pedosphere. Doi. org/10.1016/j.pedsph.2023.09.008.
[39] Wang, J., Wang, H., Zhang, R., Wei, L., Cao, R., Wang, L., et al., 2022. Variations of nitrogen-metabolizing enzyme activity and microbial community under typical loading conditions in full-scale leachate anoxic/aerobic system. Bioresour Technol 351, 126946.
[40] Wang, Y., Bai, Y., Su, J., Ali, A., Gao, Z., Huang, T., et al., 2023. Advances in microbially mediated manganese redox cycling coupled with nitrogen removal in wastewater treatment: A critical review and bibliometric analysis. Chem Eng J 461, 141878.
[41] Wood, D.E., Lu, J., Langmead, B., 2019. Improved metagenomic analysis with Kraken 2. Genome Biol 20, 257.
[42] Xiang, H., Hong, Y., Wu, J., Wang, Y., Ye, F., Ye, J., et al., 2023. Denitrification contributes to N_2O emission in paddy soils. Front Microbiol 14, 1–13.
[43] Xiu, W., Lloyd, J., Guo, H., Dai, W., Nixon, S., Bassil, N.M., et al., 2020. Linking microbial community composition to hydrogeochemistry in the western Hetao Basin: Potential importance of ammonium as an electron donor during arsenic mobilization. Environ Int 136, 105489.
[44] Xu, B., Shi, L., Zhong, H., Wang, K., 2021. Investigation of Fe(II) and Mn(II) involved anoxic denitrification in agricultural soils with high manganese and iron contents. J Soil Sediment 21, 452–468.
[45] Xu, C., Zhu, H., Wang, J., Ji, C., Liu, Y., Chen, D., et al., 2023. Fertilizer N triggers native soil N-derived N_2O emissions by priming gross N mineralization. Soil Biol Biochem 178, 108961.
[46] Xu, J.J., Zhu, X.L., Zhang, Q.Q., Cheng, Y.F., Xu, L.Z.J., Zhu, Y.H., et al., 2018. Roles of MnO_2 on performance, sludge characteristics and microbial community in anammox system. Sci Total Environ 633, 848–856.
[47] Yan, W.W., Sun, F.Q., Liu, J.B., Zhou, Y., 2018. Enhanced anaerobic phenol degradation by conductive materials via EPS and microbial community alteration. Chem Eng J 352, 1–9.
[48] Yi, B., Wang, H., Zhang, Q., Jin, H., Abbas, T., Li, Y., et al., 2019. Alteration of gaseous nitrogen losses via anaerobic ammonium oxidation coupled with ferric reduction from paddy soils in Southern China. Sci Total Environ 652, 1139–1147.
[49] Yuan, C., Li, Q., Sun, Z., Zhang, W., Chen, J., Chen, Z., et al., 2023. Chemical oxidation of arsenic in the environment and its application in remediation: A mini review. Pedosphere 33, 185–193.
[50] Zhang, C., Xiao, X., Zhao, Y., Zhou, J., Sun, B., Liang, Y., 2021. Patterns of microbial arsenic detoxification genes in low-arsenic continental paddy soils. Environ Res 201, 111584.
[51] Zhang, F., Chen, Y., Zhao, F., Yuan, P., Lu, M., Qin, K., et al., 2023. Use of magnetic powder to effectively improve the denitrification employing the activated sludge fermentation liquid as carbon source. J Environ Manag 348, 119049.
[52] Zhang, H., Yuan, X., Xiong, T., Wang, H., Jiang, L., 2020. Bioremediation of co-contaminated soil with heavy metals and pesticides: Influence factors, mechanisms and evaluation methods. Chem Eng J 398, 125657.
[53] Zhang, M., Li, Z., Häggblom, M.M., Young, L., He, Z., Li, F., et al., 2020. Characterization of nitrate-dependent As(III)-oxidizing communities in arsenic-contaminated soil and investigation of their metabolic potentials by the combination of DNA-stable isotope probing and metagenomics. Environ Sci Technol 54, 7366–7377.
[54] Zhao, C., Zhang, J., Chen, Z., Li, J., Shu, L., Ji, X., 2022. Effective constructions of electro-active bacteria-derived bioelectrocatalysis systems and their applications in promoting extracellular electron transfer process. Prog Chem 34, 397–410.
[55] Zhao, Y., Zhang, Xx, Zhao, Z., Duan, C., Chen, H., Wang, M., et al., 2018. Metagenomic analysis revealed the prevalence of antibiotic resistance genes in the gut and living environment of freshwater shrimp. J Hazard Mater 350, 10–18.